

# YIELD-DRIVEN EM OPTIMIZATION USING SPACE MAPPING-BASED NEUROMODELS

J.W. Bandler, J.E. Rayas-Sánchez and Q.J. Zhang  
Simulation Optimization Systems Research Laboratory  
and Department of Electrical and Computer Engineering  
McMaster University, Hamilton, Canada L8S 4K1

Tel 905 628 9671 Fax 905 628 1578 Email j.bandler@ieee.org

## ***Abstract***

In this work, an efficient procedure to realize electromagnetics-based yield optimization and statistical analysis of microwave structures using space mapping-based neuromodels is proposed. Our technique is illustrated by the EM-based statistical analysis and yield optimization of an HTS microstrip filter. In our paper we demonstrate the use of neuromappings for both symmetric and asymmetric tolerance variations.

## ***Introduction***

With the increasing availability of commercial EM simulators, it is very desirable to include them in statistical analysis and yield-driven design of microwave circuits. Given the high cost in computational effort imposed by the EM simulators, creative procedures must be searched to efficiently use them for statistical analysis and design.

For the first time, we propose the use of space mapping-based neuromodels for efficient and accurate EM-based statistical analysis and yield optimization of microwave structures. In the full paper, we briefly review the use of neural networks for the design by optimization of microwave circuits and we mathematically formulate the yield optimization problem using SM-based neuromodels. Here, a general equation to express the relationship between the fine and coarse model sensitivities through a nonlinear, frequency-sensitive neuromapping is presented. We illustrate our technique by the yield analysis and optimization of a high-temperature superconducting (HTS) quarter-wave parallel coupled-line microstrip filter.

## ***Yield Analysis and Optimization via Space Mapping Based Neuromodels***

Let the vectors  $\mathbf{x}_c, \mathbf{x}_f \in \mathfrak{X}^n$  represent the design parameters of the coarse and fine models, respectively. The operating frequency  $\omega$ , used by the fine model, can be different to that used by the coarse model  $\omega_c$ . Let  $\mathbf{R}_c(\mathbf{x}_c, \omega_c), \mathbf{R}_f(\mathbf{x}_f, \omega) \in \mathfrak{R}^r$  represent the coarse and fine model responses at  $\omega_c$  and  $\omega$ , respectively. We denote the corresponding SM-based neuromodel responses at frequency  $\omega$  as  $\mathbf{R}_{SMBN}(\mathbf{x}_f, \omega)$ , given by

$$\mathbf{R}_{SMBN}(\mathbf{x}_f, \omega) = \mathbf{R}_c(\mathbf{x}_c, \omega_c) \quad (1)$$

with

$$\begin{bmatrix} \mathbf{x}_c \\ \omega_c \end{bmatrix} = \mathbf{P}(\mathbf{x}_f, \omega) \quad (2)$$

where the mapping function  $\mathbf{P}$  is implemented by a neural network following any of the 5 neuromapping variations (SM, FDSM, FSM, FM or FPSM) described in [1]. We assume that a suitable mapping function  $\mathbf{P}$  has already been found (i.e., a neural network with suitable complexity has already been trained).

If the SM-based neuromodel is properly developed,

$$\mathbf{R}_f(\mathbf{x}_f, \omega) \approx \mathbf{R}_{SMBN}(\mathbf{x}_f, \omega) \quad (3)$$

for all  $\mathbf{x}_f$  and  $\omega$  in the training region.

Let the Jacobian of the fine model responses w.r.t. the fine model parameters be  $\mathbf{J}_f \in \mathfrak{R}^{r \times n}$ ; let the Jacobian of the coarse model responses w.r.t. the coarse model parameters and mapped frequency be  $\mathbf{J}_c \in \mathfrak{R}^{r \times (n+1)}$  and let the Jacobian of the mapping w.r.t. the fine model parameters be  $\mathbf{J}_p \in \mathfrak{R}^{(n+1) \times n}$ . Then the sensitivities of the fine model responses can be approximated using

$$\mathbf{J}_f \approx \mathbf{J}_c \mathbf{J}_p \quad (4)$$

The accuracy of the approximation of  $\mathbf{J}_f$  using (4) will depend on how well the SM-based neuromodel reproduces the behavior of the fine model in the training region.

---

This work was supported in part by the Natural Sciences and Engineering Research Council of Canada (NSERC) under Grants OGP0007239, STR234854-00 and through the Micronet Network of Centres of Excellence. J.W. Bandler is also with Bandler Corporation, P.O. Box 8083, Dundas, Ontario, Canada L9H 5E7. Q.J. Zhang is with the Department of Electronics, Carleton University, 1125 Colonel By Drive, Ottawa, Canada K1S 5B6.

If the mapping is implemented with a 3-layer perceptron with  $h$  hidden neurons, (2) is given by

$$\mathbf{P}(\mathbf{x}_f, \boldsymbol{\omega}) = \mathbf{W}^o \boldsymbol{\Phi}(\mathbf{x}_f, \boldsymbol{\omega}) + \mathbf{b}^o \quad (5)$$

$$\boldsymbol{\Phi}(\mathbf{x}_f, \boldsymbol{\omega}) = [\varphi(s_1) \quad \varphi(s_2) \quad \dots \quad \varphi(s_h)]^T \quad (6)$$

$$\mathbf{s} = \mathbf{W}^h \begin{bmatrix} \mathbf{x}_f \\ \boldsymbol{\omega} \end{bmatrix} + \mathbf{b}^h \quad (7)$$

where  $\mathbf{W}^o \in \mathfrak{R}^{(n+1) \times h}$  is the matrix of output weighting factors,  $\mathbf{b}^o \in \mathfrak{R}^{n+1}$  is the vector of output bias elements,  $\boldsymbol{\Phi} \in \mathfrak{R}^h$  is the vector of hidden signals,  $\mathbf{s} \in \mathfrak{R}^h$  is the vector of activation potentials,  $\mathbf{W}^h \in \mathfrak{R}^{h \times (n+1)}$  is the matrix of hidden weighting factors,  $\mathbf{b}^h \in \mathfrak{R}^h$  is the vector of hidden bias elements and  $h$  is the number of hidden neurons. A typical choice for the nonlinear activation functions is hyperbolic tangents, i.e.,  $\varphi(\cdot) = \tanh(\cdot)$ . All the internal parameters of the neural network,  $\mathbf{b}^o$ ,  $\mathbf{b}^h$ ,  $\mathbf{W}^o$  and  $\mathbf{W}^h$  are constant since the SM-based neuromodel has been already developed.

The Jacobian  $\mathbf{J}_P$  is obtained from (5-7) as

$$\mathbf{J}_P = \mathbf{W}^o \mathbf{J}_\phi \mathbf{W}^h \quad (8)$$

where  $\mathbf{J}_\phi \in \mathfrak{R}^{h \times h}$  is a diagonal matrix given by  $\mathbf{J}_\phi = \text{diag}(\varphi'(s_j))$ , with  $j = 1 \dots h$ . If the SM-based neuromodel uses a 2-layer perceptron, the Jacobian  $\mathbf{J}_P$  is simply

$$\mathbf{J}_P = \mathbf{W}^o \quad (9)$$

which corresponds to the case of a frequency-sensitive linear mapping. Notice that by substituting (9) in (4) and assuming a frequency-insensitive neuromapping we obtain the lemma found in [2], since in the case of a 2-layer perceptron with no frequency dependance,  $\mathbf{W}^o \in \mathfrak{R}^{n \times n}$ .

### ***Yield Optimization of an HTS Filter (Symmetric Case)***

Consider a high-temperature superconducting (HTS) parallel coupled-line microstrip filter [1, 3] (Fig. 1). OSA90/hope™ built-in linear elements connected by circuit theory form the “coarse” model. Sonnet’s *em*™ driven by Empipe™ forms the fine model, using a high-resolution grid. The SM-based neuromodel of the HTS filter of [3] is used. The corresponding SM-based neuromodel is illustrated in Fig. 2, which implements a frequency partial-space mapped neuromapping with 7 hidden neurons, mapping only  $L_1$ ,  $S_1$  and the frequency (3LP:7-7-3). Applying direct minimax optimization to the coarse model, we obtain the optimal coarse solution  $\mathbf{x}_c^*$ . We apply direct minimax optimization to the SM-based neuromodel, starting at  $\mathbf{x}_c^*$ , to obtain the optimal SM-based neuromodel nominal solution  $\mathbf{x}_{SMBN}^*$ .

For yield analysis, we consider 0.2% of variation for the dielectric constant and for the loss tangent, as well as 75 micron of variation for the physical dimensions, with uniform statistical distributions. We perform Monte Carlo yield analysis of the SM-based neuromodel around  $\mathbf{x}_{SMBN}^*$  with 500 outcomes. This takes a few tens of seconds on a PC (AMD 640MHz, 256M RAM, Windows NT 4.0). A single outcome calculation for the same circuit using an EM simulation takes about 5 hours. The responses for 50 outcomes are shown in Fig. 3. The yield calculation is shown in Fig. 4. A yield of only 18.4% is obtained at  $\mathbf{x}_{SMBN}^*$ . We then apply yield optimization to the SM-based neuromodel with 500 outcomes using the Yield-Huber optimizer available in OSA90/hope™, obtaining the optimal yield solution:  $\mathbf{x}_{SMBN}^{y*}$ . The corresponding responses for 50 outcomes are shown in Fig. 5. The yield is increased from 18.4% to 66%, as shown in Fig. 6.

### ***Conclusions***

An efficient procedure to realize EM-based statistical analysis and yield optimization of microwave structures using space mapping-based neuromodels is proposed. A general equation to express the relationship between the fine and coarse model sensitivities through a nonlinear, frequency-sensitive neuromapping is presented. In the full paper we show a creative procedure to avoid the need of extra EM simulations when asymmetric variations in the physical parameters due to tolerances are considered, by re-using the available neuromappings on asymmetric coarse models.

### ***References***

- [1] M.H. Bakr, J.W. Bandler, M.A. Ismail, J.E. Rayas-Sánchez and Q.J. Zhang, “Neural space mapping optimization for EM-based design,” *IEEE Trans. Microwave Theory Tech.*, vol. 48, 2000, pp. 2307-2315.
- [2] M.H. Bakr, J.W. Bandler, N. Georgieva and K. Madsen, “A hybrid aggressive space-mapping algorithm for EM optimization,” *IEEE Trans. Microwave Theory Tech.*, vol. 47, 1999, pp. 2440-2449.
- [3] J.W. Bandler, M.A. Ismail, J.E. Rayas-Sánchez and Q.J. Zhang, “Neuromodeling of microwave circuits exploiting space mapping technology,” *IEEE Trans. Microwave Theory Tech.*, vol. 47, 1999, pp. 2417-2427.

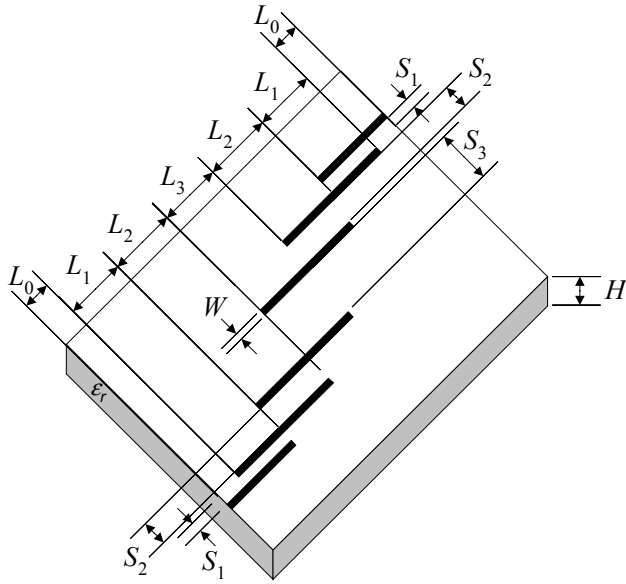


Fig. 1. HTS quarter-wave parallel coupled-line microstrip filter.

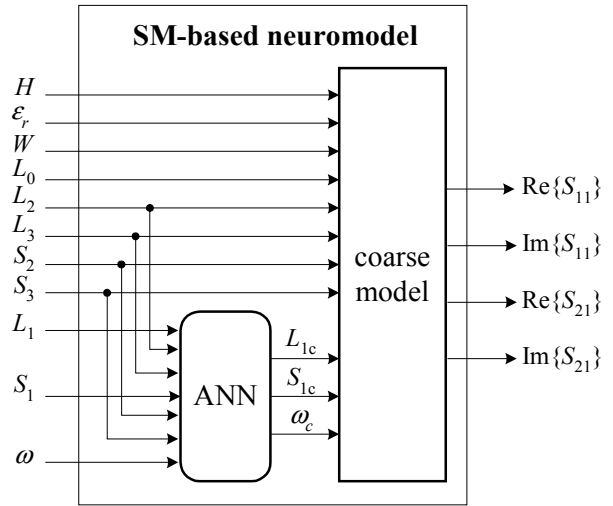


Fig. 2. SM-based neuromodel of the HTS filter for yield analysis assuming symmetry ( $L_{1c}$  and  $S_{1c}$  correspond to  $L_1$  and  $S_1$  as used by the coarse model).

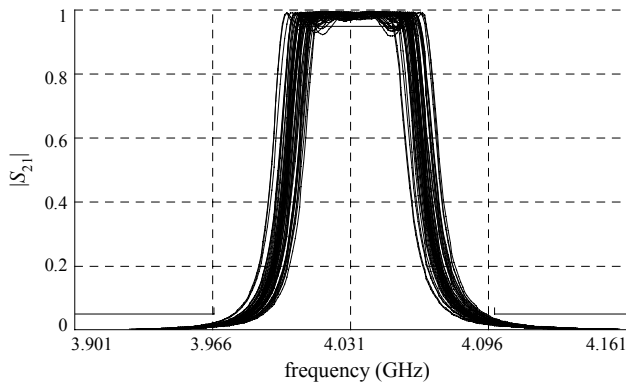


Fig. 3. Monte Carlo yield analysis of the SM-based neuromodel responses around the optimal nominal solution  $\mathbf{x}_{SMBN}^*$  with 50 outcomes.

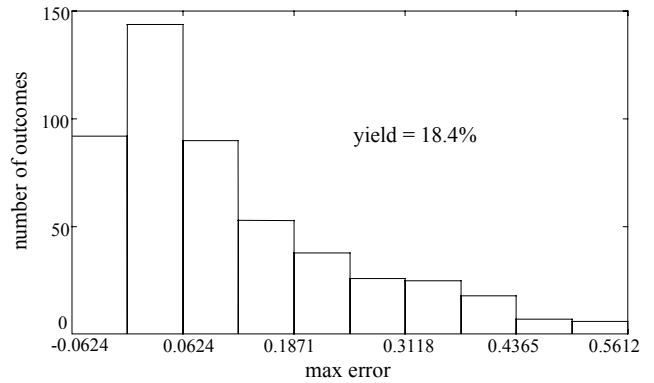


Fig. 4. Histogram of the yield analysis of the SM-based neuromodel around the optimal nominal solution  $\mathbf{x}_{SMBN}^*$  with 500 outcomes.

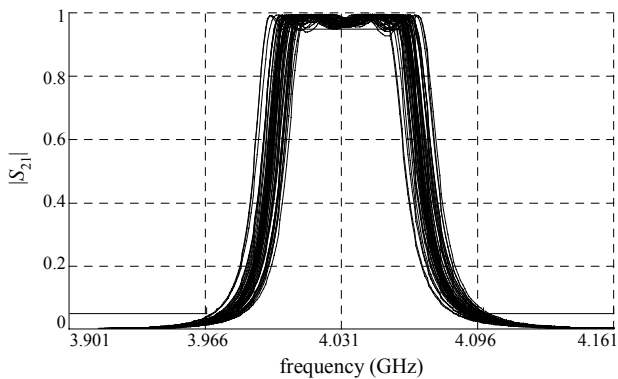


Fig. 5. Monte Carlo yield analysis of the SM-based neuromodel responses around the optimal yield solution  $\mathbf{x}_{SMBN}^{y*}$  with 50 outcomes.

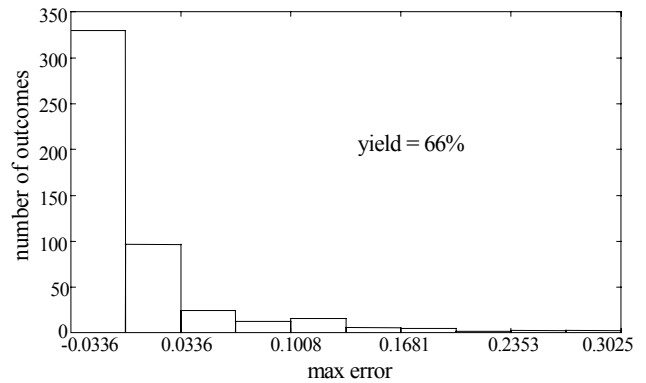


Fig. 6. Histogram of the yield analysis of the SM-based neuromodel around the optimal yield solution  $\mathbf{x}_{SMBN}^{y*}$  with 500 outcomes (considering symmetry).